WILEY InterScience® DISCOVER SOMETHING GREAT

# Revisiting the Geometry of $nd^{10}$ $(n+1)s^0$ $[M(H_2O)]^{p+}$ Complexes Using Four-Component Relativistic DFT Calculations and Scalar Relativistic Correlated CSOV Energy Decompositions ($M^{p+}$ = $Cu^+$, $Zn^{2+}$, $Ag^+$, $Cd^{2+}$, $Au^+$, $Hg^{2+}$)

**CHRISTOPHE GOURLAOUEN,[1] JEAN-PHILIP PIQUEMAL,[2] TROND SAUE,[3] OLIVIER PARISEL[1]**

[1]*Laboratoire de Chimie Théorique, UMR 7616 CNRS/UPMC, Université Pierre et Marie Curie, Case courier 137 - 4, place Jussieu, F. 75252 Paris, France*

[2]*Laboratory of Structural Biology, National Institute of Environmental Health Science, Mail Drop F0-08, P.O Box 12233, Research Triangle Park, North Carolina 27709*

[3]*Laboratoire de Chimie Quantique et Modélisation Moléculaire, UMR 7551 CNRS/ULP, Université Louis Pasteur, Institut Le Bel, 4, rue Blaise Pascal, F. 67000 Strasbourg, France*

*Received 9 June 2005; Accepted 17 August 2005*
*DOI 10.1002/jcc.20329*
*Published online in Wiley InterScience (www.interscience.wiley.com).*

**Abstract:** Hartree–Fock and DFT (B3LYP) nonrelativistic (scalar relativistic pseudopotentials for the metallic cation) and relativistic (molecular four-component approach coupled to an all-electron basis set) calculations are performed on a series of six $nd^{10}$ $(n+1)s^0$ $[M(H_2O)]^{p+}$ complexes to investigate their geometry, either planar $C_{2v}$ or nonplanar $C_s$. These complexes are, formally, entities originating from the complexation of a water molecule to a metallic cation: in the present study, no internal reorganization has been found, which ensures that the complexes can be regarded as a water molecule interacting with a metallic cation. For $[Au(H_2O)]^+$ and $[Hg(H_2O)]^{2+}$, it is observed that both electronic correlation and relativistic effects are required to recover the $C_s$ structures predicted by the four-component relativistic all-electron DFT calculations. However, including the zero-point energy corrections makes these shallow $C_s$ minima vanish and the systems become floppy. In all other systems, namely $[Cu(H_2O)]^+$, $[Zn(H_2O)]^{2+}$, $[Ag(H_2O)]^+$, and $[Cd(H_2O)]^{2+}$, all calculations predict a $C_{2v}$ geometry arising from especially flat potential energy surfaces related to the out-of-plane wagging vibration mode. In all cases, our computations point to the quasi-perfect transferability of the atomic pseudopotentials considered toward the molecular species investigated. A rationalization of the shape of the wagging potential energy surfaces (i.e., single well vs. double well) is proposed based on the Constrained Space Orbital Variation decompositions of the complexation energies. Any way of stabilizing the lowest unoccupied orbital of the metallic cation is expected to favor charge-transfer (from the highest occupied orbital(s) of the water ligand), covalence, and, consequently, $C_s$ structures. The CSOV complexation energy decompositions unambiguously reveal that such stabilizations are achieved by means of relativistic effects for $[Au(H_2O)]^+$, and, to a lesser extent, for $[Hg(H_2O)]^{2+}$. Such analyses allow to numerically quantify the *rule of thumb* known for $Au^+$ which, once again, appears as a better archetype of a relativistic cation than $Hg^{2+}$. This observation is reinforced due to the especially high contribution of the nonadditive correlation/relativity terms to the total complexation energy of $[Au(H_2O)]^+$.

© 2005 Wiley Periodicals, Inc. J Comput Chem 27: 142–156, 2006

**Key words:** relativistic effects; four-component relativistic calculations; CSOV decomposition analysis; scalar relativistic pseudopotentials

## Introduction

Heavy metal cations are known to be involved in biological processes,[1,2] usually as poisons. Properly controlled or chelated, they may however act as drugs. For example, the poisoning effect of mercury has been known for a long time, but quicksilver salts have been used as worm powder at least until the late 18th century; mercuric oxyde still is used in pharmacology as a great ophthalmic antiseptic. Colloidal gold is an oligoelement that helps in cicatrisation processes; gold is also used as Auranofin®, a divalent

***Correspondence to:*** O. Parisel; e-mail: parisel@lct.jussieu.fr

Contract/grant sponsor: the Intramural Research Program of the NIH (J.-P. P.)

Contract/grant sponsor: NIEHS (J.-P. P.)

© 2005 Wiley Periodicals, Inc.

phosphinegold(I) thiolate to treat some forms of rheumatisms such as arthritis.[3] Silver, either colloidal or cationic, has antiseptic and antibiotic properties.

The behavior of such metals in biological environments is not always clearly established at the molecular level. It is thus of interest to model the complexes that these elements or their cations can make to determine how they may act *in vivo*. As it is well known that even slight geometrical distortions of an enzymatic active site or slight modifications of its energetic properties can dramatically modify, enhance, or inhibit the role of a protein, such knowledge is especially important.

The physical chemistry involved in biological processes usually implies, in its key steps, only slight structural changes and/or low-energy reaction paths: it is thus necessary to validate the theoretical methodologies that could be applied to large systems by comparing them with results obtained from high-level *ab initio* calculations on model systems that have proven to quantitatively account for such perturbations.

A first step in such investigations is thus the modeling of the interaction of heavy cations with small species representative of the chemical functions encountered in biological systems. In this article, we will restrict ourselves to the most abundant of these molecules, namely water, and will report the structural properties of the $[M(H_2O)]^+$ (M = Cu, Ag, Au) and $[M(H_2O)]^{2+}$ (M = Zn, Cd, Hg) species. Within this set of species, all cations share the same external $nd^{10}$ $(n+1)s^0$ electronic ground state configuration.

Two different problems must be taken into account. The first one is the well-known role of electronic correlation effects on the complexation energies and on the geometries. The second one comes from the fact that, because some of these cations have a large nuclear charge, relativistic effects could be strong enough to significantly affect physicochemical properties.[4–12] [A recent state-of-the-art presentation of computational and theoretical relativistic chemistry can be found in the Special Issue of *Chemical Physics*, dedicated to the memory of Dr. Bernd A. Heß: Chem. Phys. 311 (2005).]

Up to now, the combined effects of correlation and relativity have been taken into account by coupling relativistic pseudopotentials to standard correlated methods. However, to the best of our knowledge, no molecular four-component correlated relativistic all-electron calculations have been performed on the six complexes mentioned above. We have thus found of interest to carry out such CPU-expensive reference calculations and to compare them with cheaper scalar relativistic pseudopotential computations. In this way, it might be possible to distinguish the respective roles of relativity and correlation and to unambiguously and firmly establish the relevance of using the Density Functional Theory (DFT) combined with one-component relativistic pseudopotentials, an approach that may easily be applicable to larger systems.

In this work, we will compare results given by scalar relativistic calculations performed using all-electron or pseudopotential basis sets to results obtained from all-electron four-component relativistic calculations. We will also provide some insights into the covalent or electrostatic nature of the binding between $M^{p+}$ and $H_2O$ by means of complexation energy decompositions and try to relate them to the preferred geometry adopted by each complex.

## Computational Procedures

The scalar relativistic calculations have been performed using the GAUSSIAN03 package[13] within the Restricted Hartree–Fock (RHF) and B3LYP formalisms. The standard 6-31+G** basis sets were used to describe the O and H atoms, whereas scalar relativistic pseudopotentials (PP) were used for the heavy atoms.[14] These are either the LANL2DZ PP by Hay and Wadt[15] coupled to a double-zeta quality basis set, or the small-core relativistic so-called SDD pseudopotentials by Dolg et al.[16,17] coupled to a double-zeta quality basis set obtained from a (8s7p6d)/[6s5p3d] contraction. For the sake of comparison with another high-quality pseudopotential, we have also investigated the Averaged Relativistic Effective PP (AREP)[18–20] known in the EMSL database under the CRENBL acronym.* The valence basis sets associated to these PPs, which have been optimized on neutral atoms for LANL2DZ and CRENBL, and on *quasi-neutral* atoms for SDD, are used as such with the following contraction patterns. For the LANL2DZ, the valence electrons are taken as $ns^2$ $np^6$ $nd^{10}$ $(n+1)s^0$ and the corresponding primitives and contractions are (8s6p4d)/[3s3p2d] for $Cu^+$ ($n = 3$), $Ag^+$ ($n = 4$), $Au^+$ ($n = 5$), (3s2p5d)/[2s2p2d] for $Zn^{2+}$ ($n = 3$), and (3s3p4d)/[2s2p2d] for $Cd^{2+}$ ($n = 4$). For $Hg^{2+}$ ($n = 5$) the valence is reduced to the $5d^{10}$ $6s^0$ levels, which are described using a (3s3p3d)/[2s2p2d] contraction. For the SDD pseudopotentials, the valence is defined as $ns^2$ $np^6$ $nd^{10}$ $(n+1)s^0$ for all cations. The contraction used is (8s7p6d)/[6s5p3d] for all cations but $Au^+$ and $Hg^{2+}$ for which (8s6p5d)/[7s3p4d] and (8s8p7d)/[6s6p4d] respective contractions are used. The CRENBL pseudopotentials used here consider the same valence as SDD and a totally uncontracted basis set, (5s5p4d)/[5s5p4d], whatever the cation.

The All-Electron (AE) calculations have been performed using the uncontracted Faegri's basis sets on the heavy atoms; these basis sets are known to be of at least double-zeta quality.[21] No supplementary polarization functions were added. Still, the standard 6-31+G** basis sets were used to describe O and H.

The calculations have been performed using the DIRAC code,[22] which has been recently extended to the Density Functional Theory formalism.[23,24] The nonrelativistic four-component RHF and B3LYP calculations have been performed using the Lévy-Leblond Hamiltonian.[25] The four-component relativistic calculations, RHF and B3LYP, were based on the Dirac–Coulomb Hamiltonian,[26] and will hereafter be referred to as, respectively, DHF (Dirac–Hartree–Fock) and DB3LYP (Dirac-B3LYP). The uncontracted small component basis sets were generated from the large component sets according to the strict kinetic balance condition. Finite size Gaussian nuclei were used and the nuclear exponents were taken from a list a values recommended by Viss-

*This basis set was obtained from the Extensible Computational Chemistry Environment Basis Set Database, Version 02/25/04, as developed and distributed by the Molecular Science Computing Facility, ***E****nvironmental and* ***M****olecular* ***S****ciences* ***L****aboratory*, which is part of the Pacific Northwest Laboratory, P.O. Box 999, Richland, WA 99352, and funded by the U.S. Department of Energy. The Pacific Northwest Laboratory is a multiprogram laboratory operated by Battelle Memorial Institute for the U.S. Department of Energy under contract DE-AC06-76RLO 1830. http://www.emsl.pnl.gov/forms/basisform.html.)

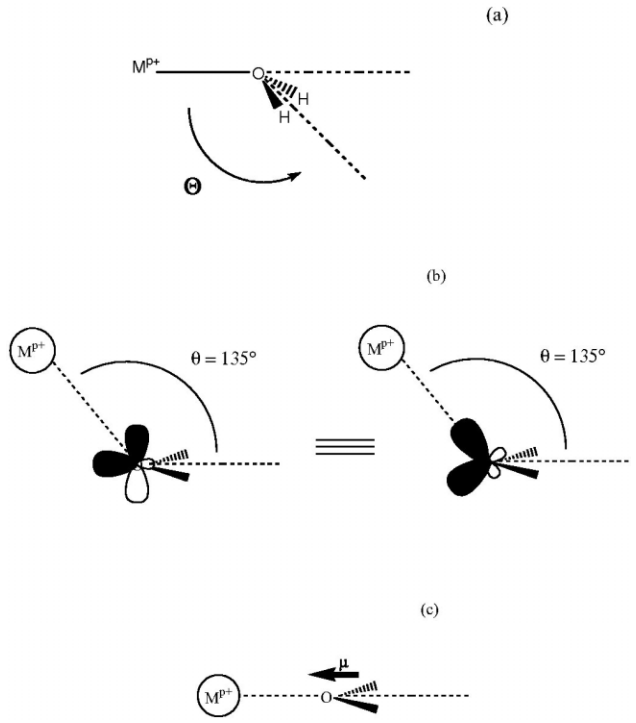


**Figure 1.** (a) Definition of the dihedral angle Θ characterizing the out-of-plane wagging deformation in the $[M(H_2O)]^{p+}$ complexes. This angle corresponds to the angle between the M—O axis and the bisecting axis of the HOH valence angle. (b) "Orbital control": (left) most efficient overlap with canonical orbitals (Θ = 135°), (right) corresponding hybrids ("rabbit ears"); (c) "electrostatic control": most efficient interaction between the cation charge and the water dipole (Θ = 180°).

cher and Dyall.[27] All (SS/SS) and (SS/LL) type integrals have been explicitly retained in the calculations.

Moreover, some scalar relativistic correlated (MP2) second-order Douglas–Kroll–Heß (DKH2) calculations[28–31] have also been performed as implemented in GAUSSIAN03.

NBO (Natural Bonding Orbitals) analyses[32] have been performed according to the implementation made in GAUSSIAN03.

Full geometry optimizations have been performed for the complexes considered, always starting from a $C_s$ structure (Fig. 1a) allowed to relax to the $C_{2v}$ symmetry characterized by a (M O H H) dihedral angle Θ equal to 180.0°. The variations of this angle are indicative of the wagging out-of-plane deformation of the system (*pyramidalization*). All optimizations using pseudopotentials rely on analytical gradients as well as the RHF and DHF all-electron approaches. The B3LYP/AE and DB3LYP/AE optimizations have used a numerical gradient.

The nature of the calculated stationary points has been characterized by a vibrational analysis performed within the harmonic approximation. The normal modes will thereafter be labeled as follows: $\omega$ for the wagging out-of-plane mode, $\beta$ for the HOH bending mode, $\rho$ for the M—O stretching mode, $\kappa$ for the rocking mode, $\sigma_-$ and $\sigma_+$, respectively, for the antisymmetric and symmetric stretching modes of the OH bonds. No scaling procedure has been applied and the vibrational frequencies were used as such to evaluate the Zero-Point-Energy (ZPE) corrections:

$$\delta E_{\mathrm{ZPE}} = \mathrm{ZPE(complex)} - \mathrm{ZPE}(H_2O).$$

The complexation energies used hereafter are defined according to:

$$\Delta E = E(\mathrm{complex}) - E(\mathrm{cation}) - E(H_2O) = -D_e.$$

The Basis Set Superposition Error (BSSE) to $\Delta E$ has been determined according to the counterpoise procedure which gives the correction as:[33,34]

$$\delta E_{BSSE} = E_A[\mathbf{r}_{AB},\{\chi_A\}] + E_B[\mathbf{r}_{AB},\{\chi_A\}U\{\chi_B\}] - E_B[\mathbf{r}_{AB},\{\chi_A\}U\{\chi_B\}]$$

where $\mathbf{r}_{\mathrm{AB}}$ stands for the equilibrium geometry of the AB complex, $\{\chi_{\mathrm{A}}\}$ and $\{\chi_{\mathrm{B}}\}$ for the basis set of fragment A and fragment B, respectively, and $\{\chi_{\mathrm{A}}\}\ U\ \{\chi_{\mathrm{B}}\}$ for the full basis set of AB. $E_{\mathrm{A}}$ and $E_{\mathrm{B}}$ are the energies computed according to the specified geometry and basis set.

This leads to the final value, $D_0$:

$$D_0 = D_e - \delta E_{\mathrm{ZPE}} + \delta E_{\mathrm{BSSE}}.$$

The complexation energy decompositions have been performed using a modified version of HONDO95.3[35] as explained below.

## Results

### $[Ag(H_2O)]^+$

Although several experimental investigations of this complex have been performed, they have not been devoted to the elucidation of the exact structure of this system, but were limited to the evaluation of the binding energy.[36–38] However, many calculations have been performed, using various levels of *ab initio* chemistry approaches:[37,39–48] in most cases a $C_{2v}$ structure was hypothesized. Only in refs. 44 and 46 and $C_s$ and $C_{2v}$ geometries are explicitly considered; unfortunately, when the $C_s$ structure is found as the lowest energy structure, which occurs for some methods, the value of Θ is not reported.

It should be pointed out that all previous calculations were limited to relativistic approaches relying on various kinds of pseudopotentials, except for the work by Antušek et al.,[49] who have used a one-component relativistic approach within spin-averaged DKH method on the neutral $[Ag(H_2O)]$ complex, and, very recently the spin-averaged DKH2/MP2/AE calculations performed on $[Ag(H_2O)]^+$.[50]

As seen from Table 1, a very nice agreement is observed between the DB3LYP/AE and the B3LYP/PP approaches for the structural parameters and for the complexation energy. The B3LYP/SDD value of −31.6 kcal/mol for $\Delta E$ (as well as the −30.8 kcal/mol value at the B3LYP/CRENBL level of calculations) is in almost perfect agreement with the DB3LYP/AE result. LANL2DZ performs the worst. The computed $D_e$ value is in good

**Table 1.** Geometrical Parameters (Å and Degrees) and Complexation Energy (kcal/mol) for the $[Ag(H_2O)]^+$ Complex.

| | Pseudopotential approach | | | | | | All-electron approach | | | |
|---|---|---|---|---|---|---|---|---|---|---|
| | CRENBL | | LANL2DZ | | SDD | | Nonrelativistic | | Relativistic | |
| | RHF | B3LYP[a] | RHF | B3LYP | RHF | B3LYP[b] | RHF | B3LYP | DHF | DB3LYP |
| r(Ag-O) | 2.353 | 2.240 | 2.368 | 2.266 | 2.342 | 2.229 | 2.401 | 2.300 | 2.349 | 2.237 |
| r(OH) | 0.948 | 0.968 | 0.948 | 0.968 | 0.948 | 0.969 | 0.948 | 0.968 | 0.948 | 0.965 |
| b(HOH) | 107.1 | 107.9 | 107.1 | 107.6 | 107.1 | 107.9 | 106.7 | 106.6 | 106.9 | 107.4 |
| Θ | 180.0 | 177.2 | 180.0 | 173.5 | 180.0 | 176.7 | 180.0 | 180.0 | 180.0 | 177.3 |
| $\Delta E$ | −24.5 | −30.8 | −24.0 | −29.5 | −24.9 | −31.6<br>−30.4[c] | −23.6 | −28.7 | −24.8 | −31.5 |

[a]Vibrational frequencies ($cm^{-1}$): 148 ($\omega$), 315 ($\rho$), 545 ($\kappa$), 1640 ($\beta$), 3786 ($\sigma_+$), 3887 ($\sigma_-$).
[b]Vibrational frequencies ($cm^{-1}$): 120 ($\omega$), 315 ($\rho$), 548 ($\kappa$), 1639 ($\beta$), 3782 ($\sigma_+$), 3883 ($\sigma_-$).
[c]BSSE corrected.

agreement with the experimental results: 33.3 ± 2.2 kcal/mol,[36] or more recently, 1.37 ± 0.11 eV (31.6 ± 2.53 kcal/mol).[37] Due to the computational cost required to estimate the ZPE at the DB3LYP/AE level, we have evaluated it at the B3LYP/SDD level: it amounts to 14.7 kcal/mol for the complex and to 13.4 kcal/mol for the water molecule (the vibrational frequencies are: 1604, 3809, and 3930 $cm^{-1}$). This correction gives 30.3 kcal/mol, which is further reduced to $D_0$ = 29.5 kcal/mol when the BSSE correction is included. This value is still in good agreement with the experimental value mentioned above.

It also appears (Table 1) that the AE calculations predict a $C_{2v}$ geometry if either relativity or correlation is neglected. When both effects are taken into account, a slight divergence from $C_{2v}$ towards $C_s$ is observed. The same trend is observed from PP calculations: only the B3LYP/PP approach recovers a $C_s$ structure. Such a departure from $C_{2v}$ remains, however, very limited: it does not exceed 6.5° (B3LYP/LANL2DZ). The DB3LYP calculation yields a divergence by 2.7°, which is significantly weaker than the 18.2° found by DKH2/MP2/AE calculations,[50] although the associated complexation energy (1.36 eV, 31.3 kcal/mol) remains almost unchanged. We have performed DKH2/MP2/AE calculations on this system using the all-electron basis set described above, and have not been able to reproduce such a large divergence from $C_{2v}$: we get Θ = 179.9° in agreement with the DB3LYP/AE and B3LYP/PP calculations given in Table 1. However, the Potential Energy Surface (PES) relative to the variation of Θ is very flat (Fig. 2), and any change in the computational procedure (basis set, level of relativistic approximation, number of correlated electrons, level of correlation used) might be responsible for changes in the optimized geometry. At the B3LYP/SDD level, the one mimicking the DB3LYP/AE calculations the best, no transition state for Θ = 180° nor any energy barrier could be found. In fact, the PES relative to the $\omega$ mode is especially flat (Fig. 2), and thus favors a large amplitude movement. At the equilibrium geometry, a NBO analysis reveals that the OH bonds might be seen as $sp^{2.65}$ hybrids, the axial bonding orbital to a $sp^{1.2}$ hybrid, and the remaining lone pair as a pure 2p orbital orthogonal to the $C_2$ axis.

The Ag—O bond length is decreased by both the correlation (RHF/AE vs. B3LYP/AE: −0.101 Å, which is very close to the analogous RHF/SDD vs. B3LYP/SDD value of −0.113 Å) and relativistic effects (RHF/AE vs. DHF/AE: −0.052 Å). No cooperativity is observed because the variation between DB3LYP/AE and RHF/AE amounts to −0.164 Å, very close to the total of −0.153 Å arising from the previous two-term decomposition. In the present case, the decrease of the bond length due to correlation when going from RHF/AE to DB3LYP/AE is about two-thirds, whereas the one due to relativity amounts to one-third.

### $[Au(H_2O)]^+$

Previous works on this complex share the same characteristics as for $[Ag(H_2O)]^+$: experimental investigations have measured the binding energy[51–55] but did not consider the geometry. A number of calculations have been performed, using various scalar relativistic approaches of *ab initio* chemistry.[42,49,51,55–58]

As seen from Table 2 and Figure 3, the $C_s$ structure can be recovered only if both correlation and relativistic effects are taken

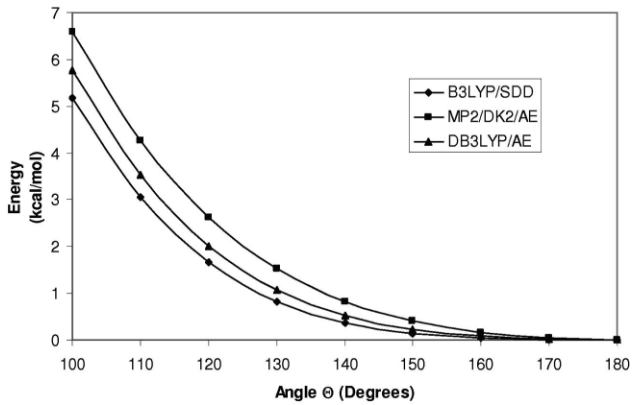


**Figure 2.** Wagging potential energy curve as a function of Θ (see text for definition) for the $[Ag(H_2O)]^+$ complex (all-electron four-component relativistic: DB3LYP, scalar relativistic one-component: B3LYP/SDD, all-electron scalar relativistic two-component: DKH2/MP2/AE).

**Table 2.** Geometrical Parameters (Å and Degrees) and Complexation Energy (kcal/mol) for the $[Au(H_2O)]^+$ Complex.

| | Pseudopotential approach | | | | | | All-electron approach | | | |
|---|---|---|---|---|---|---|---|---|---|---|
| | CRENBL | | LANL2DZ | | SDD | | Nonrelativistic | | Relativistic | |
| | RHF | B3LYP[a] | RHF | B3LYP | RHF | B3LYP[b] | RHF | B3LYP | DHF | DB3LYP |
| r(Au-O) | 2.287 | 2.174 | 2.301 | 2.191 | 2.300 | 2.177 | 2.481 | 2.389 | 2.258 | 2.137 |
| r(OH) | 0.948 | 0.972 | 0.948 | 0.972 | 0.948 | 0.972 | 0.948 | 0.969 | 0.948 | 0.972 |
| b(HOH) | 108.3 | 108.3 | 108.2 | 108.2 | 108.4 | 108.3 | 106.5 | 106.7 | 108.2 | 109.0 |
| Θ | 180.0 | 136.8 | 180.0 | 137.1 | 180.0 | 137.3 | 180.0 | 180.0 | 180.0 | 138.7 |
| $\Delta E$ | −27.0 | −38.8 | −26.3 | −37.2 | −26.8 | −38.7<br>−37.4[c] | −22.1 | −27.0 | −27.9 | −41.2 |

[a]Vibrational frequencies ($cm^{-1}$): 346 ($\rho$), 451 ($\omega$), 693 ($\kappa$), 1622 ($\beta$), 3736 ($\sigma_+$), 3839 ($\sigma_-$).
[b]Vibrational frequencies ($cm^{-1}$): 346 ($\rho$), 447 ($\omega$), 693 ($\kappa$), 1624 ($\beta$), 3733 ($\sigma_+$), 3838 ($\sigma_-$).
[c]BSSE corrected.

into account. Whatever the basis sets used (AE or PP), neglecting either the correlation (RHF and DHF calculations) or neglecting relativity (RHF and B3LYP) leads to a planar $C_{2v}$ structure. The dihedral Θ angle obtained at the DB3LYP/AE level of calculation amounts to 138.7°. This value can be reproduced using the less elaborate B3LYP/LANL2DZ (137.1°) and B3LYP/SDD (137.3°) methods. The Θ = 138.7° value compares favorably with the 43.7° value (Θ = 136.3°) obtained from DKH2/MP2/AE calculations.[50] Moreover, the Au—O bond length of 2.177 Å obtained with the B3LYP/SDD approach is in good agreement with the reference value of 2.137 Å obtained at DB3LYP/AE level. The B3LYP/LANL2DZ value is slightly too large (2.191 Å), which might be another clue that the SDD potentials should be more appropriate. The CRENBL pseudopotentials behave like SDD.

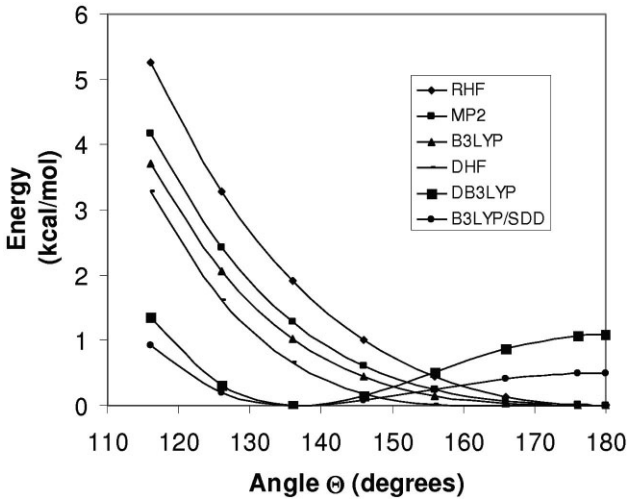


**Figure 3.** Wagging potential energy curves as a function of Θ (see text for definition) for the $[Au(H_2O)]^+$ complex (B3LYP/SDD and all-electron calculations: four-component relativistic for DHF and DB3LYP, scalar relativistic one-component for RHF, MP2, and B3LYP).

At the equilibrium geometry, an NBO analysis reveals that the OH bonds might be seen as $sp^{2.2}$ hybrids. The water bonding orbital pointing towards $Au^+$ has only 16% s-character (and thus 84% p-character). The remaining lone pair has 22% s-character and 78% p-character.

The Au—O bond length is decreased by both the correlation (RHF/AE vs. B3LYP/AE: −0.092 Å) and, very significantly, by relativistic effects (RHF/AE vs. DHF/AE: −0.223 Å). Such a large change due to relativity has also been observed for the neutral [Au(—$H_2O$)] complex.[49] No significant cooperativity appears, as the variation between DB3LYP/AE and RHF/AE amounts to −0.344 Å, very close to the total of −0.315 Å obtained from the previous two-term decomposition. In $[Au(H_2O)]^+$, correlation contributes roughly only one-third in the decrease of the bond length while relativity contributes the remaining two-thirds: these respective contributions are reversed when compared to the *less relativistic* $[Ag(H_2O)]^+$ complex.

The computed DB3LYP/AE reference value for the complexation energy amounts to −41.2 kcal/mol. Again, because of the computational cost required to estimate the ZPE correction at the DB3LYP/AE level, we have evaluated it at the B3LYP/SDD level. The ZPE amounts to 15.3 kcal/mol for the complex: this gives a theoretical reference DB3LYP/AE $D_0$ value of 39.3 kcal/mol, which is in excellent agreement with the experimental $D_0$ value of 1.74 ± 0.1 eV (40.1 ± 2.3 kcal/mol).[53–55]

The B3LYP/SDD $D_e$ complexation energy of 38.7 kcal/mol is closer to the reference DB3LYP/AE value of 41.2 kcal/mol than that obtained from B3LYP/LANL2DZ (37.2 kcal/mol). SDD and CRENBL still perform better than LANL2DZ with respect to the reference value. It gives $D_0$ = 36.8 kcal/mol, which reduces to 35.5 kcal/mol when accounting for the BSSE corrections.

The most accurate DB3LYP/AE calculations indicate that the planar $C_{2v}$ structure is a transition state with respect to the $\omega$ mode: the transition barrier is 1.08 kcal/mol. Including the ZPE corrections obtained from B3LYP/SDD calculations reduces the height of the barrier down to 0.43 kcal/mol (150 $cm^{-1}$). For this transition state, the vibrational wave numbers are: *336i* ($\omega$), 347 ($\rho$), 630 ($\kappa$), 1610 ($\beta$), 3764 ($\sigma_+$) and 3879

**Table 3.** Geometrical Parameters (Å and Degrees) and Complexation Energy (kcal/mol) for the $[Hg(H_2O)]^{2+}$ Complex.

| | Pseudopotential approach | | | | | | All-electron approach | | | |
|---|---|---|---|---|---|---|---|---|---|---|
| | CRENBL | | LANL2DZ | | SDD | | Nonrelativistic | | Relativistic | |
| | RHF | B3LYP[a] | RHF | B3LYP | RHF | B3LYP[b] | RHF | B3LYP | DHF | DB3LYP |
| r(Hg-O) | 2.140 | 2.146 | 2.174 | 2.214 | 2.143 | 2.150 | 2.263 | 2.231 | 2.116 | 2.112 |
| r(OH) | 0.961 | 0.989 | 0.960 | 0.982 | 0.961 | 0.989 | 0.958 | 0.979 | 0.961 | 0.989 |
| b(HOH) | 109.1 | 109.4 | 108.3 | 108.9 | 109.2 | 109.2 | 106.2 | 107.7 | 108.9 | 109.6 |
| Θ | 180.0 | 139.1 | 180.0 | 155.2 | 180.0 | 137.6 | 180.0 | 180.0 | 180.0 | 138.2 |
| $\Delta E$ | −72.4 | −92.9 | −69.3 | −75.5 | −72.5 | −93.7<br>−92.3[c] | −59.7 | −69.7 | −73.8 | −95.6 |

[a]Vibrational frequencies ($cm^{-1}$): 393 ($\rho$), 580 ($\omega$), 840 ($\kappa$), 1599 ($\beta$), 3515 ($\sigma_+$), 3611 ($\sigma_-$).
[b]Vibrational frequencies ($cm^{-1}$): 396 ($\rho$), 602 ($\omega$), 846 ($\kappa$), 1597 ($\beta$), 3507 ($\sigma_+$), 3604 ($\sigma_-$).
[c]BSSE corrected.

($\sigma_-$) $cm^{-1}$. B3LYP/SDD still gives a barrier of 0.50 kcal/mol, which, in fact, disappears if the ZPE corrections are taken into account (−0.15 kcal/mol).

Due to the very small energy difference between the $C_{2v}$ and $C_s$ structures, it appears difficult to firmly establish what would be the observed geometry in high-level rotational or vibrational spectroscopic works. Either the barrier is high enough to have the complex trapped in a well-defined $C_s$ minimum (the potential would thus consist in a double well), or the barrier does not exist and the species will thus be observed as a fluxional entity exhibiting a large wagging amplitude. (The theoretical treatment of such structures is detailed in refs. 59a,b. The landmark books by G. Herzberg,[59c] H. W. Kroto,[59d] and E. B. Wilson et al.[59e] are starting references for that topic.) Although the harmonic approximation used to evaluate this out-of-plane vibration may not be reliable due to the very shallow potential, it should be pointed out that the corresponding wave number (447 $cm^{-1}$) will make the system very difficult to be trapped in the well as the barrier is overcome as soon as the second vibrational level is reached.

### *$[Hg(H_2O)]^{2+}$*

Investigations on the gas-phase $[Hg(H_2O)]^{2+}$ complex are not very common from both the experimental and theoretical points of view. RHF/PP calculations have been performed assuming a $C_{2v}$ symmetry.[60] A semiempirical treatment has also been employed.[61] More recently, a comparison between the $C_s$ and $C_{2v}$ structures has been carried out at the B3LYP, MP2, and QCISD levels relying either on LANL2DZ or ECP60MWB pseudopotentials:[62] a $C_s$ structure was predicted, with Θ varying between 141.7° and 151.4° with respect to the PP used.

As seen from Table 3 and Figure 4, a $C_s$ structure is found when both relativity and correlation effects are taken into account. The reference four-component DB3LYP/AE calculation predicts Θ = 138.2°; the B3LYP/CRENBL and B3LYP/SDD approaches are in very nice agreement with this value (139.1° and 137.6°, respectively). DKH2/MP2/AE calculations have shown to give the close value of Θ = 140.6°.[50]

At the equilibrium geometry, a NBO analysis reveals that the OH bonds might be seen as $sp^{2.13}$ hybrids. The water bonding orbital pointing towards $Hg^{2+}$ has only 9.5% s-character (and thus 90.5% p-character). The remaining lone pair has 27% s-character and 73% p-character. The natural bonding orbitals are thus close to those observed in $[Au(H_2O)]^+$, although the s-character of the bonding $Hg^{2+}$–$H_2O$ orbital is slightly less pronounced.

The DB3LYP/AE complexation energy of −95.6 kcal/mol is fairly well reproduced by the PP approaches (CRENBL: −92.9 and SDD: −93.7 kcal/mol). In contrast, the B3LYP/LANL2DZ results are in poor agreement with the reference calculations: Θ = 155.2° and $\Delta E$ = −75.5 kcal/mol. Including the BSSE correction for the B3LYP/SDD calculation gives: $D_e$ = 92.3 kcal/mol. Including the ZPE correction reduces this value to $D_0$ = 90.6 kcal/mol.

The Hg—O bond length amounts to 2.112 Å at the four-component DB3LYP/AE level of calculation and to 2.263 Å at the

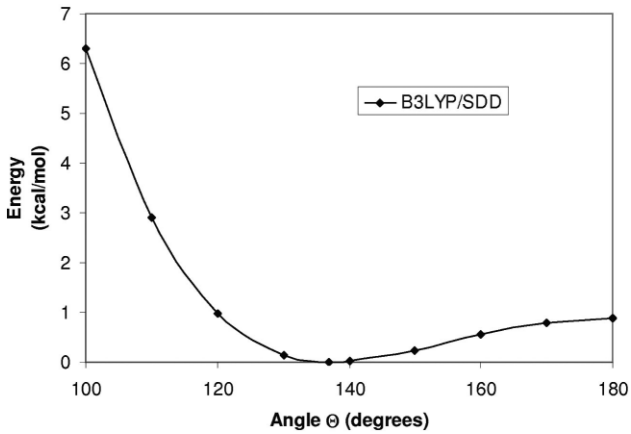


**Figure 4.** Wagging potential energy curve as a function of Θ (see text for definition) for the $[Hg(H_2O)]^{2+}$ complex (B3LYP/SDD calculations).

four-component RHF/AE level: this gives a total increase of −0.151 Å. The decrease due to correlation (RHF/AE vs. B3LYP/AE) amounts to −0.032 Å and that due to relativity (RHF/AE vs. DHF/AE) amounts to −0.147 Å; their sum is −0.179 Å. We here observe what could be called an anticooperative effect between correlation and relativity on this bond length. However, the role of relativistic effects on the bond length is largely predominant. At the B3LYP/SDD level of calculations, the $C_{2v}$ structure appears to be a transition state having the following wave numbers: *456i* ($\omega$), 439($\rho$), 794($\kappa$), 1581($\beta$), 3544($\sigma_+$), and 3657 ($\sigma_-$) $cm^{-1}$. The barrier amounts to 0.9 kcal/mol, which reduces to 0.1 kcal/mol when the ZPE corrections are taken into account. With the DB3LYP/AE approach, the electronic barrier amounts to 0.6 kcal/mol, adding the ZPE corrections makes it disappear, as was the case for $[Au(H_2O)]^+$.

In contrast with the $Ag^+$ and $Au^+$ complexes, $[Hg(H_2O)]^{2+}$ may not be observable in the gas-phase: charge-transfer between $M^{2+}$ and $H_2O$ may occur, leading to $M^+$ and $H_2O^+$, followed by a rapid Coulomb explosion. Whether the $[Hg(H_2O)]^{2+}$ species is subject, or not, to such a phenomenon depends on the relative position of the $Hg^+$–$H_2O^+$ and $Hg^{2+}$–$H_2O$ potential energy surfaces. The theoretical treatment is challenging, and should rely on multireference wave functions because a careful examination of the crossing occurring between the relevant open-shell (singlet and triplet) and close-shell (singlet) potential energy surfaces is required. Such an investigation is beyond the scope of this article.

**Table 4.** Energy Decompositions (kcal/mol), Correlation vs. Relativity and Nonadditivity (AE and PP Approaches).

| | $[Ag(H_2O)]^+$ | $[Au(H_2O)]^+$ | $[Hg(H_2O)]^{2+}$ |
|---|---|---|---|
| | | AE | |
| $E_0$ | −23.6 | −22.1 | −59.7 |
| $E_c$ | −5.1 | −4.9 | −10.0 |
| $E_r$ | −1.2 | −5.7 | −14.1 |
| $E_{rc}^{ex}$ | −7.9 | −19.1 | −35.9 |
| $E_{rc}^{na}$ | −1.6 | −8.5 | −11.8 |
| $E_{rc}^{na}/\Delta E$ | 5.7% | 20.6% | 12.5% |
| $E_0 + E_r$ | −24.8 | −27.8 | −73.8 |
| $E_c + E_{rc}^{na}$ | −6.7 | −13.4 | −21.8 |
| | | SDD | |
| $E_0$ | −24.9 | −26.8 | −72.5 |
| $E_c$ | −6.7 | −11.9 | −21.1 |
| | | CRENBL | |
| $E_0$ | −24.5 | −27.0 | −72.4 |
| $E_c$ | −6.3 | −11.8 | −20.5 |

## Discussion on the AE and PP Approaches

### *On the Nonadditivity of Relativity and Correlation in AE Calculations*

As shown in a previous section when dealing with bond lengths, it appears that correlation and relativistic effects may not be additive. Nonadditive effects have been investigated for a number of molecules, for example, in the dihalogens,[63] hydrogen halides,[64] and interhalogen[65] series, or in water and ammonia complexes of coinage metals.[49] To investigate the respective role of correlation and relativity in the total complexation energy $\Delta E$, as well as to estimate nonadditivity effects, a very simple energy decomposition was performed. It relies on the following expression, where the $\Delta E$ (DB3LYP/AE) value, considered as the reference, is built from independent relativistic and correlation contributions added to the well-defined RHF/AE level of approximation:

$$\Delta E(\text{DB3LYP/AE}) = E_0 + E_{rc}^{ex}$$
$$E_0 = \Delta E(\text{RHF/AE})$$
$$E_{rc}^{ex} = E_c + E_r + E_{rc}^{na}$$

$E_{rc}^{ex}$ is the exact contribution from relativity and correlation. $E_c$ is the contribution issued from pure correlation, $E_r$, that corresponding to pure relativity. $E_{rc}^{na}$ is a nonadditive coupled relativity–correlation term.

We here use the following decomposition to estimate "pure correlation" and "pure relativity" contributions:

$$E_c = \Delta E(\text{B3LYP/AE}) - E_0$$
$$E_r = \Delta E(\text{DHF/AE}) - E_0$$

The nonadditive term can therefore be expressed as:

$$E_{rc}^{na} = +[\Delta E(\text{DB3LYP/AE}) - \Delta E(\text{B3LYP/AE}) - \Delta E(\text{DHF/AE}) + \Delta E(\text{RHF/AE})].$$

As seen from Table 4, the contribution of $E_r$ increases going from $Ag^+$ to $Hg^{2+}$ through $Au^+$, but a clear nonadditivity of the correlation and relativistic effects is observed. $E_{rc}^{na}$ amounts to 5.7% of $\Delta E$(DB3LYP/AE) for $Ag^+$ and increases to 12.5% for $Hg^{2+}$. Gold, still, exhibits a remarkable behaviour as the nonadditivity increases to more than 20%.

### *On the Reliability of the DFT/PP Approach*

#### *Structures and Complexation Energies*

As detailed in the previous section (Tables 1, 2, and 3), there is an almost perfect agreement between the four-component DB3LYP/AE calculations and the B3LYP/PP approach if using SDD or CRENBL pseudopotentials. This agreement is found for both the complexation energies and the geometries, especially for the M—O bond lengths and for the out-of-plane wagging $\Theta$ angles. The LANL2DZ pseudopotentials perform well for $[Ag(H_2O)]^+$ and $[Au(H_2O)]^+$, but appear unreliable for $[Hg(H_2O)]^{2+}$, when dealing with both $\Theta$ and, more dramatically, $\Delta E$. This is not really surprising as, for Hg, the valence is in that case limited to the 5d and 6s levels, which are described by a relatively small (2s2p2d) contraction.

**Table 5.** Orbital (or Spinor) Absolute Energies (a.u.) for the Water Molecule $3a_1$ and $1b_1$ Lone Pairs and the $5s^0$ ($Ag^+$) or $6s^0$ ($Au^+$ and $Hg^{2+}$) Cations.

| | Pseudopotential approach | | | | | | All-electron approach | | | |
|---|---|---|---|---|---|---|---|---|---|---|
| | CRENBL | | LANL2DZ | | SDD | | Nonrelativistic | | Relativistic | |
| | RHF | B3LYP | RHF | B3LYP | RHF | B3LYP | RHF | B3LYP | DHF | DB3LYP |
| $H_2O$ ($3a_1$) | −0.581 | −0.394 | −0.581 | −0.394 | −0.581 | −0.394 | −0.581 | −0.391 | −0.581 | −0.391 |
| $H_2O$ ($1b_1$) | −0.510 | −0.321 | −0.510 | −0.321 | −0.510 | −0.321 | −0.510 | −0.318 | −0.510 | −0.317 |
| $Ag^+$ (5s) | −0.230 | −0.389 | −0.229 | −0.378 | −0.231 | −0.393 | −0.214 | −0.361 | −0.230 | −0.386 |
| $Au^+$ (6s) | −0.274 | −0.452 | −0.277 | −0.445 | −0.274 | −0.452 | −0.214 | −0.363 | −0.275 | −0.452 |
| $Hg^{2+}$ (6s) | −0.618 | −0.819 | −0.606 | −0.751 | −0.621 | −0.822 | −0.528 | −0.703 | −0.623 | −0.823 |

Conventions have been chosen so that the pure $2p_O$ lone pair on the oxygen atom of the water molecule belongs to the $B_1$ irreducible representation of the $C_{2v}$ group.

### *The Highest Valence (n+1)$s^0$ Level*

Table 5 shows the absolute energy of the highest valence $5s^0$ ($Ag^+$) or $6s^0$ ($Au^+$ or $Hg^{2+}$) levels. Still, for $Ag^+$ and, to a lesser extent for $Au^+$, an almost perfect agreement is observed between the PP and the AE results, regardless of the computational approach used. Whereas the agreement is retained for the SDD and CRENBL pseudopotentials if dealing with $Hg^{2+}$, a significant error is observed when using LANL2DZ: for example, the 6s level computed using B3LYP/LANL2DZ is located at −0.751 a.u., whereas the DB3LYP/AE approach locates the corresponding $6s_{1/2}$ spinor at −0.823 a.u. (−0.819 and −0.822 a.u. for CRENBL and SDD, respectively). Accordingly, the LANL2DZ pseudopotential does not emerge as the most appropriate pseudopotential to describe the $Hg^{2+}$ cation.

### *On the Correlation Recovered from Scalar Relativistic Pseudopotentials*

As relativistic effects are intrinsically included in PP calculations, only a correlation contribution can be defined for such approaches:

$$\Delta E(\text{B3LYP/PP}) = E_0 + E_c$$
$$E_0 = \Delta E(\text{RHF/PP})$$
$$E_c = \Delta E(\text{B3LYP/PP}) - E_0.$$

The numerical results are shown in Table 4. The two PP considered (SDD and CRENBL) give very close value for $E_c$, thus recovering about the same amount of correlation energy for the three complexes investigated. Of course, comparing these values to the $E_c$ values recovered from AE calculations is not relevant. Because the relativity effect is included in the $E_0$ value when dealing with PP, we thus have to compare $E_0$(PP) to $[E_0 + E_r]$(AE): as seen from Table 4, there is then an excellent agreement between these two quantities whatever the complex considered (the differences do not exceed 1 kcal/mol). We then have to compare $E_c$(PP) with the remaining components of $\Delta E$(AE), namely $[E_c + E_{rc}^{na}]$ (AE): still, a nice agreement is observed. It follows from these two comparisons that the pseudopotentials considered are able to quantitatively account for relativity and correlation effects, including the nonadditivity term, which, in PP calculations, is recovered together with the correlation energy. This provides another hint about the high quality of the SDD and CRENBL pseudopotentials and their transferability from atomic to molecular systems.

### *The $C_s$ vs. $C_{2v}$* Dilemma

Our results lead to a number of questions. Especially, in view of the small barriers (1 kcal/mol or less) recovered at the correlated/relativistic levels of calculations, but that disappear when ZPE contributions are taken into account, is it reasonable to consider that the electronic minima corresponding to $C_s$ structures are really minima? In the following subsections, we will develop arguments that should confirm that $C_s$ structures have effectively been characterized on the basis of purely electronic calculations, even though the vibrational corrections can have the barriers between the $C_s$ and the $C_{2v}$ structures vanish.

### *The "Rule of Thumb"*

The fact that a $C_s$ structure can exist for $[Au(H_2O)]^+$ has been qualitatively explained[56–58] in terms of the increase of the electrophilic character of the 6s level of $Au^+$, which is especially subject to relativistic effects.[7,10,66,67] The lowering of this level induced by relativistic effects should make it become more susceptible to accept charge–transfer from oxygen, and thus to covalent bonding: the system would be under orbital control. This was qualitatively corroborated by mean of a simple point-charge model: the Coulombic part of the interaction between $Au^+$ and $H_2O$ was found to decrease by 9 kcal/mol going from the planar to the bent structure.[56]

The transfer from the oxygen atom should be less efficient for $Ag^+$, which implies, for that case, that the interaction would be governed by electrostatic effects, which are maximized when the water molecule dipole is directed toward the $Ag^+$ cation: the system is under charge control. The $Hg^{2+}$ cation should behave as $Au^+$. For neutral mercury, this phenomenon is experimentally observed: $Hg(6s^2\text{-}X^1S_0)$ makes long-range weakly bound van der Waals complexes, whereas the excited states arising from the

$6s^1 6p^1$ configuration ($^3P$) are highly bound and highly reactive states[68–70] in which the partially occupied 6s orbital has recovered some (high) electrophilicity.

Moreover, due to the contraction of the 6s level, which is known to be larger for gold than for mercury[7,12,66,67] the diffuseness of this level is most certainly reduced: this also contributes to increase the $\langle 6s|3a_1\rangle$ and $\langle 6s|1b_1\rangle$ overlaps involved in the charge–transfer phenomenon.

### *The* $C_s$ vs. $C_{2v}$ Dilemma: A Qualitative Rationalization

The four-component B3LYP/AE and DB3LYP/AE calculations show (Table 5) that the $Au^+$ 6s level is lowered by 0.089 a.u. (2.4 eV) due to relativity, whereas the lowering for the $Ag^+$ 5s level is limited to 0.025 a.u. (0.7 eV). The $Hg^{2+}$ cation exhibits a stronger lowering of its 6s level (0.120 a.u., 3.27 eV). In both $Au^+$ and $Hg^{2+}$, a covalent complex with $H_2O$ is thus to be favored with respect to an electrostatic complex. In these cases, and due to the spherical symmetry of the electronic distributions of these strongly electrophilic cations that both can be seen as "relativistic proton" models, the preferred angle for the approach of the cation towards water[71] corresponds to $\Theta = 135°$, which maximizes the overlap between the external empty 6s orbital and the $3a_1$ and $1b_1$ lone pairs of water (Fig. 1b). The DB3LYP/AE geometry optimizations give: 138.7° and 138.2° for $[Au(H_2O)]^+$ and $[Hg(H_2O)]^{2+}$, respectively. For $Ag^+$, the relativistic stabilization of the 5s level seems not to be large enough to have the charge–transfer, and thus covalence, increased because $\Theta$ remains about 177°, which corresponds to the case where electrostatics dominates (Fig. 1c); the corresponding potential energy surface is, however, particularly flat.

### *The* $C_s$ vs. $C_{2v}$ Dilemma: A Quantitative Rationalization

To further rationalize this rule of thumb, we have found of interest to perform energy decompositions within the CSOV[72,73] (Constrained Space Orbital Variation) framework. It is then possible to split the complexation energy $\Delta E$ of two interacting fragments A and B into different components, namely:

$$\Delta E = E_1 + E_2 + \delta E$$

where:

$$E_1 = E_{FC} = E_s + E_{Pauli}$$

$$E_2 = E_{pol} + E_{ct} = E_{polA} + E_{polB} + E_{ctA\rightarrow B} + E_{ctB\rightarrow A}$$

$$\delta E = \Delta E - E_1 - E_2$$

$E_1$, also called $E_{FC}$ where FC stands for Frozen Core, is the sum of the electrostatic ($E_s$) and the exchange/Pauli repulsion terms. $E_2$ is the sum of a charge transfer ($E_{ct} = E_{ctA\rightarrow B} + E_{ctB\rightarrow A}$) term and of a polarization ($E_{pol} = E_{polA} + E_{polB}$) term, which both can be split into contributions originating from A (water) and B (metal cation) for $E_{pol}$ and from the donation from A to B together with that of B from A for $E_{ct}$. $\delta E$ accounts for some many-body terms having different physical origin[74–77] and are not considered in the standard CSOV decomposition because they are expected to be small compared to $\Delta E$. It is important to point out that in the definition used here for $\delta E$ we also include some technical, but negligible, artefacts arising when going from a computational code to another. More precisely, this deals especially with the fact that GAUSSIAN does not handle linear dependencies arising from the basis set, whereas HONDO does.

With such a decomposition, it is possible to establish what is the leading origin of the complexation energy; this makes then possible to characterize the complex as a *covalent* ($E_2$ dominates in this case) or as an *electrostatic* ($E_1$ dominant) species. We thus introduce the weight of the electrostatic component defined as:

$$\mathbf{E} = E_1/\Delta E.$$

Here, the CSOV scheme has been applied at the B3LYP/SDD and B3LYP/CRENBL level of calculations because these approaches mimic the DB3LYP/AE results the best, and because, to the best of our knowledge, no energy decomposition scheme is available for four-component calculations. Although the applications of the CSOV decomposition are not that usual within the framework of the Kohn–Sham formalism, some examples have been published that validate such an approach.[78–81] Very recently, applications have been carried out on a set of systems stabilized from either van der Waals or electrostatic interactions.[82]

Unfortunately, it turned out that, at least in the version of HONDO we used, there is no handling of h (l = 5) spherical harmonics so that the energy decomposition for $[Hg(H_2O)]^{2+}$ could not be performed using the exact SDD pseudopotential: we have used a modified pseudopotential (SDD*) in which the h component has been removed.

As seen from Table 6 for $[Au(H_2O)]^+$, **E** values do not exceed 10% using CRENBL, and even falls to less than 4% using SDD. This complex is thus clearly covalent: it exhibits a strong charge–transfer from the water ligand, together with strong polarizations of each interacting entities.

The result of the CSOV decomposition for $[Ag(H_2O)]^+$ is astounding. Whatever the PPs used, **E** exceeds 46%. We here recall that the various methodologies investigated up to now oscillate/hesitate between a $C_{2v}$ geometry and a $C_s$ structure characterized by a high "out-of-plane" $\Theta$ angle (varying between a minimum of 162° found at the DKH2/MP2/AE level of calculations[50] and a maximum of 177.3° found in this work using the DB3LYP AE approach). The CSOV decomposition indeed shows that there is here a strong competition between $E_1$ and $E_2$, and thus between a covalent and an ionic/electrostatic complex: this might be a clear illustration that the transition between the $C_{2v}$ and $C_s$ structures for this kind of $nd^{10}$ $(n+1)s^0$ complexes occurs for $n$ = 4, which corresponds to the $Ag^+$ cation. This might also explain why the PES relative to the $\omega$ mode found for $[Ag(H_2O)]^+$ is so flat (see earlier and Fig. 2).

**E** falls to 29.5% (CRENBL) or 31.7% (SDD*) for $[Hg(H_2O)]^{2+}$: as was found for $[Au(H_2O)]^+$, covalence effects are the largest and an electronically stable $C_s$ equilibrium structure can be obtained. No significant differences are found in the results between CRENBL and SDD*.

**Table 6.** CSOV Energy Decompositions (kcal/mol) of the B3LYP/PP Calculations.

| | $[Ag(H_2O)]^+$ | | $[Au(H_2O)]^+$ | | | $[Hg(H_2O)]^{2+}$ | | |
|---|---|---|---|---|---|---|---|---|
| | CRENBL $C_{2v}$ | SDD $C_{2v}$ | CRENBL $C_s$ | SDD $C_s$ | CRENBL[a] $C_{2v}$ | CRENBL $C_s$ | SDD* $C_s$ | CRENBL[b] $C_{2v}$ |
| $\Delta E$ | −30.8 | −31.6 | −38.8 | −38.7 | −38.4 | −92.9 | −93.7 | −92.3 |
| $E_s$ | −43.03 | −43.76 | −57.34 | −54.92 | −58.11 | −76.76 | −76.92 | −81.51 |
| $E_{\text{Pauli}}$ | 26.69 | 28.80 | 53.45 | 53.63 | 52.81 | 49.33 | 47.19 | 52.55 |
| $E_1 = E_{\text{FC}}$ | −16.34 | −14.96 | −3.89 | −1.29 | −5.30 | −27.43 | −29.73 | −28.96 |
| $E_{\text{polB}}$ | −2.73 | −2.79 | −7.32 | −7.63 | −7.27 | −3.54 | −3.02 | −3.83 |
| $E_{\text{polA}}$ | −6.52 | −6.53 | −8.88 | −8.16 | −8.96 | −22.79 | −23.25 | −23.60 |
| $E_{\text{ctA}\rightarrow\text{B}}$ | −5.27 | −6.51 | −15.72 | −16.19 | −14.20 | −34.08 | −33.73 | −31.61 |
| $E_{\text{ctB}\rightarrow\text{A}}$ | −0.66 | −0.45 | −0.77 | −0.76 | −0.96 | −0.28 | −0.63 | −0.37 |
| $E_2$ | −15.18 | −16.27 | −32.69 | −32.74 | −31.38 | −60.70 | −60.58 | −59.43 |
| $\delta E$ | 0.72 | −0.37 | −2.22 | −4.67 | −1.72 | −4.77 | −3.39 | −3.91 |
| **E** | 53.1% | 47.3% | 10.0% | 3.3% | 13.8% | 29.5% | 31.7% | 31.4% |

"A" stands for water and "B" for the metallic cation.
[a]Constrained optimization forcing planarity: r(Au-O) = 2.164 Å, r(OH) = 0.969 Å, b(HOH) = 124.7°; vibrational frequencies ($cm^{-1}$): $\omega$ = 322i, $\rho$ = 347, $\kappa$ = 635, $\beta$ = 1611, $\sigma_+$ = 3764, $\sigma_-$ = 3878.
[b]Constrained optimization forcing planarity: r(Hg-O) = 2.118 Å, r(OH) = 0.986 Å, b(HOH) = 123.5°; vibrational frequencies ($cm^{-1}$): $\omega$ = 427i, $\rho$ = 435, $\kappa$ = 795, $\beta$ = 1586, $\sigma_+$ = 3544, $\sigma_-$ = 3655.

Two supplementary B3LYP/CRENBL CSOV calculations have been performed to investigate if strong variations could be observed in the CSOV components when going from a $C_s$ to a $C_{2v}$ structure for $[Au(H_2O)]^+$ and $[Hg(H_2O)]^{2+}$. As seen from Table 6, **E** slightly increases for both complexes when planarity is imposed, which means that the complexes become slightly less covalent. However, comparing $E_1$ and $E_2$ in both geometries do not reveal variations superior to 2 kcal/mol. In the case of $[Au(H_2O)]^+$, $E_s$, the component certainly the most comparable to the Coulombic energy reported *supra*, varies by 0.77 kcal/mol, far from the 9 kcal/mol variation computed using a point-charge model;[56] simultaneously, $E_{\text{Pauli}}$ decreases by 0.64 kcal/mol: this results in a total reinforcement of $E_1$ by only 1.41 kcal/mol. In the same time, the weight of $E_2$ is reduced by 1.31 kcal/mol, essentially due to the $E_{\text{ctA}\rightarrow\text{B}}$ term: as expected, charge transfer from oxygen is less favorable in the $C_{2v}$ structure. Variations are more important in the case of $[Hg(H_2O)]^{2+}$: $E_s$ is reinforced by 4.75 kcal/mol when turning to the planar structure, but, simultaneously, $E_{\text{Pauli}}$ increases by 3.22 kcal/mol. This results in a partial compensation making $E_1$ slightly stronger by 1.53 kcal/mol. As for $Au^+$, $E_2$ is reduced by 1.27 kcal/mol, essentially because of the decrease of the $E_{\text{ctA}\rightarrow\text{B}}$ component, by 2.47 kcal/mol. The conclusion of this analysis is at variance with the point-charge models that very certainly overestimate the role of the electrostatic component: it is shown here that the slight increase of **E** when going to the planar form comes from the cooperative slight increase of $E_1$ and slight decrease of $E_2$. However, the weight of $E_2$ is intrinsically so high, especially because of the values of $E_{\text{polA}}$ and $E_{\text{ctA}\rightarrow\text{B}}$, and the PES is by far so flat, that it is not possible to have $E_1$ competing with $E_2$ and have the $C_{2v}$ structure favored for both these complexes.

### *The* $C_s$ *vs.* $C_{2v}$ *Dilemma: Application to* $Cu^+$, $Zn^{2+}$, *and* $Cd^{2+}$

Following the rule, it is expected that $[Cu(H_2O)]^+$ and $[Zn(H_2O)]^{2+}$ will adopt a $C_{2v}$ structure as well as, very certainly $[Cd(H_2O)]^{2+}$, because relativistic effects comparable to those existing in $Au^+$ are not expected.

Our calculations (Tables 7, 8, and 9) predict $C_{2v}$ structures as has been found by many *ab initio* calculations for $Zn^{2+}$ ($n$ = 3),[48,50,83–89] and $Cd^{2+}$ ($n$ = 4)[48,50,83,87,90] In both cases the computed complexation energies are in good agreement with other *ab initio* calculations.

The striking case appears for $[Cu(H_2O)]^+$: almost all previous calculations agree with a $C_{2v}$ structure[42,48,91–95] following the empirical rule of thumb, the previous analysis (see Table 10 for the variations of the $4s^0$ level and the validation of the pseudopotentials) and our geometry optimizations (Table 7). However, a recent DKH2/MP2/AE calculation[50] reports a $C_s$ structure with a significant $\Theta$ angle of 162°. As it has been pointed out that the MP series exhibit a poor convergence for $Cu^+$ cation complexes,[96–98] it was initially thought that the MP2 level of calculation might have been responsible for such a large angle. We have performed a DKH2/MP2/AE optimization and have found: $\Theta$ = 179.6°, which still indicates a $C_{2v}$ structure. Still, the very flat PES might be responsible for the changes observed in the optimized geometry when changing the computational procedure. Our computed $D_e$ and $D_0$ values are, however, in fair agreement with the available experimental determinations.[99]

For these three cases, it is thus to be concluded that the rule of thumb still applies. The B3LYP/SDD and B3LYP/CRENBL calculations are in excellent agreement with the four-component DB3LYP calculations. B3LYP/LANL2DZ calculations provide

**Table 7.** Geometrical Parameters (Å and Degrees) and Complexation Energy (kcal/mol) for the $[Cu(H_2O)]^+$ Complex.

| | Pseudopotential approach | | | | | | All-electron approach | | | |
|---|---|---|---|---|---|---|---|---|---|---|
| | CRENBL | | LANL2DZ | | SDD | | Nonrelativistic | | Relativistic | |
| | RHF | B3LYP[a] | RHF | B3LYP | RHF | B3LYP[b] | RHF | B3LYP | DHF | DB3LYP |
| r(Cu-O) | 2.048 | 1.926 | 2.064 | 1.961 | 2.045 | 1.935 | 2.066 | 1.952 | 2.042 | 1.923 |
| r(OH) | 0.949 | 0.969 | 0.949 | 0.969 | 0.949 | 0.970 | 0.949 | 0.970 | 0.949 | 0.971 |
| b(HOH) | 107.6 | 108.9 | 107.5 | 108.5 | 107.8 | 109.0 | 107.6 | 108.3 | 107.6 | 108.9 |
| Θ | 177.6 | 177.1 | 178.6 | 177.9 | 180.0 | 170.4 | 179.2 | 180.0 | 179.3 | 177.2 |
| $\Delta E$ | −32.0 | −42.7 | −32.3 | −40.9 | −32.8 | −43.2<br>−41.7[c] | −31.7 | −42.3 | −32.6 | −44.7 |

[a]Vibrational frequencies ($cm^{-1}$): 149 ($\omega$), 417 ($\rho$), 635 ($\kappa$), 1648 ($\beta$), 3777 ($\sigma_+$), 3872 ($\sigma_-$).
[b]Vibrational frequencies ($cm^{-1}$): 123 ($\omega$), 411 ($\rho$), 625 ($\kappa$), 1640 ($\beta$), 3768 ($\sigma_+$), 3865 ($\sigma_-$).
[c]BSSE corrected.

less comparable results. However, as seen from Figure 5, all exhibit a very flat out-of-plane wagging PES.

The relevant **E** values are shown in Table 11 and can be summarized as follows:

$$Cu^+ (37.8\%) < Zn^{2+} (43.0\%) < Cd^{2+} (45.9\%).$$

All complexes have their **E** value about 40%, and might thus be seen as slightly covalent. However, such a high value, not so far from 50%, still indicates a significant competition between covalence and electrostatics: this may result in very flat PES around $\Theta = 180°$, as observed (Fig. 5).

## Conclusions

For the six $nd^{10}$ $(n + 1)s^0$ complexes investigated in this work, it has been clearly established that B3LYP/PP calculations can perform as well as four-component DB3LYP/AE approaches for structural parameters and complexation energies. The pseudopotentials used here can be ordered by increasing quality as:

$$LANL2DZ < CRENBL \approx SDD.$$

On the basis of the molecular results presented, and also on the basis of the location of the lowest lying vacant cationic orbital, the applicability and transferability of the CRENBL and SDD pseudopotentials (initially calibrated on atoms) has been proven to be relevant to molecular species. These investigations point out to the reliability of using such PPs within a DFT treatment when dealing with large molecular systems such as those involved in biological processes.

The $[Cu(H_2O)]^+$, $[Zn(H_2O)]^{2+}$, $[Cd(H_2O)]^{2+}$, and $[Ag(H_2O)]^+$ complexes are found to be $C_{2v}$ species exhibiting large-amplitude out-of-plane wagging: this is due to especially flat potential energy surfaces. In contrast, $[Au(H_2O)]^+$ and $[Hg(H_2O)]^{2+}$ are found to be

**Table 8.** Geometrical Parameters (Å and Degrees) and Complexation Energy (kcal/mol) for the $[Zn(H_2O)]^{2+}$ Complex.

| | Pseudopotential approach | | | | | | All-electron approach | | | |
|---|---|---|---|---|---|---|---|---|---|---|
| | CRENBL | | LANL2DZ | | SDD | | Nonrelativistic | | Relativistic | |
| | RHF | B3LYP[a] | RHF | B3LYP | RHF | B3LYP[b] | RHF | B3LYP | DHF | DB3LYP |
| r(Zn-O) | 1.882 | 1.865 | 1.907 | 1.908 | 1.890 | 1.871 | 1.898 | 1.872 | 1.878 | 1.861 |
| r(OH) | 0.964 | 0.987 | 0.963 | 0.985 | 0.964 | 0.987 | 0.963 | 0.987 | 0.964 | 0.988 |
| b(HOH) | 107.5 | 109.8 | 107.4 | 108.0 | 108.2 | 110.4 | 107.2 | 109.4 | 107.8 | 110.1 |
| Θ | 179.9 | 179.5 | 179.9 | 180.0 | 179.8 | 179.9 | 178.0 | 178.2 | −179.9 | 178.0 |
| $\Delta E$ | −87.7 | −102.4 | −87.0 | −93.0 | −91.1 | −106.5<br>−105.0[c] | −88.4 | −103.7 | −90.4 | −107.2 |

[a]Vibrational frequencies ($cm^{-1}$): 253 ($\omega$), 533 ($\rho$), 817 ($\kappa$), 1643 ($\beta$), 3550 ($\sigma_+$), 3625 ($\sigma_-$).
[b]Vibrational frequencies ($cm^{-1}$): 235 ($\omega$), 532 ($\rho$), 800 ($\kappa$), 1628 ($\beta$), 3539 ($\sigma_+$), 3618 ($\sigma_-$).
[c]BSSE corrected.

**Table 9.** Geometrical Parameters (Å and Degrees) and Complexation Energy (kcal/mol) for the $[Cd(H_2O)]^{2+}$ Complex.

| | Pseudopotential approach | | | | | | All-electron approach | | | |
|---|---|---|---|---|---|---|---|---|---|---|
| | CRENBL | | LANL2DZ | | SDD | | Nonrelativistic | | Relativistic | |
| | RHF | B3LYP[a] | RHF | B3LYP | RHF | B3LYP[b] | RHF | B3LYP | DHF | DB3LYP |
| r(Cd-O) | 2.144 | 2.118 | 2.112 | 2.128 | 2.136 | 2.107 | 2.164 | 2.134 | 2.130 | 2.104 |
| r(OH) | 0.959 | 0.982 | 0.960 | 0.981 | 0.959 | 0.982 | 0.959 | 0.981 | 0.960 | 0.983 |
| b(HOH) | 107.3 | 109.6 | 106.9 | 107.3 | 107.2 | 109.5 | 106.2 | 107.7 | 106.9 | 109.1 |
| Θ | 180.0 | 179.4 | 179.9 | 180.0 | 180.0 | 179.9 | 179.8 | 178.9 | 179.1 | 177.1 |
| $\Delta E$ | −68.8 | −81.8 | −70.9 | −75.0 | −69.2 | −82.6 | −65.1 | −75.4 | −68.6 | −81.6 |
| | | | | | | −81.3[c] | | | | |

[a]Vibrational frequencies ($cm^{-1}$): 155 ($\omega$), 445 ($\rho$), 742 ($\kappa$), 1629 ($\beta$), 3608 ($\sigma_+$), 3696 ($\sigma_-$).
[b]Vibrational frequencies ($cm^{-1}$): 168 ($\omega$), 453 ($\rho$), 745 ($\kappa$), 1631 ($\beta$), 3604 ($\sigma_+$), 3690 ($\sigma_-$).
[c]BSSE corrected.

nonplanar and, as far as the sole electronic effects are concerned, retain a $C_s$ symmetry. In these cases, the $C_{2v}$ geometries are transition states with respect to out-of-plane wagging. However, the associated transition barriers are so low that they can disappear when the BSSE and/or the ZPE corrections obtained from the harmonic approximation are considered. The theoretical calculations reported in this article here reach their limitations. Such amazing results should stimulate rovibrational gas-phase, or matrix, spectroscopy experiments on these systems: provided they are not subject to Coulomb explosion, such works might allow to discriminate between a single-well potential energy surface and a surface exhibiting a double well, for which the vibrational (or even rotational) effects would be enough to cross over the pure electronic barrier and lead to wagging floppy systems.

For the static geometries obtained here (i.e., arising solely from pure electronic calculations), the *rule of thumb* that predicts $C_s$ structures for the two heaviest complexes and $C_{2v}$ structures for the lightest is obeyed. Initially formulated in the case of $Au^+$, this rule has been found reliable for $Hg^{2+}$, but less pronouncedly (maybe due to the higher cation charge), and has been rationalized by means of CSOV complexation energy decompositions: the $E_1$ energy component ("electrostatic") is dominant in the total complexation energy for all but $[Au(H_2O)]^+$ and $[Hg(H_2O)]^{2+}$, for which the $E_2$ component ("charge transfer") prevails. The investigated metallic cations involved in the $[M(H_2O)]^{p+}$ complexes can be classified according to their **E** value, which gives the following ordering at the B3LYP/SDD level of calculations:

$$Au^+ (3.3\%) < Hg^{2+} (29.5\%) < Cu^+ (37.8\%) < Zn^{2+} (43.0\%) < Cd^{2+} (45.9\%) < Ag^+ (47.3\%)$$

which can also be written as:

$$(n=5)<(n=3)<(n=4).$$

Increasing covalent character according to the CSOV analysis

Increasing covalent character according to the CSOV analysis.

In any case, favoring $E_2$ (and thus small **E**) will also favor a $C_s$ structure. One way to do this is to decrease the $(n + 1)s^0$ energy level, which will increase its electrophilic properties. This is

**Table 10.** Orbital (or Spinor) Absolute Energies (a.u.) for the Water Molecule $3a_1$ and $1b_1$ Lone Pairs and the $5s^0$ ($Cd^{2+}$) or $4s^0$ ($Cu^+$ and $Zn^{2+}$) Cations.

| | Pseudopotential approach | | | | | | All-electron approach | | | |
|---|---|---|---|---|---|---|---|---|---|---|
| | CRENBL | | LANL2DZ | | SDD | | Nonrelativistic | | Relativistic | |
| | RHF | B3LYP | RHF | B3LYP | RHF | B3LYP | RHF | B3LYP | DHF | DB3LYP |
| $H_2O$ ($3a_1$) | −0.581 | −0.394 | −0.581 | −0.394 | −0.581 | −0.394 | −0.581 | −0.391 | −0.581 | −0.391 |
| $H_2O$ ($1b_1$) | −0.510 | −0.321 | −0.510 | −0.321 | −0.510 | −0.321 | −0.510 | −0.318 | −0.510 | −0.317 |
| $Cu^+$ (4s) | −0.238 | −0.407 | −0.237 | −0.384 | −0.241 | −0.408 | −0.233 | −0.394 | −0.238 | −0.404 |
| $Zn^{2+}$ (4s) | −0.616 | −0.813 | −0.597 | −0.733 | −0.620 | −0.815 | −0.606 | −0.798 | −0.616 | −0.813 |
| $Cd^{2+}$ (5s) | −0.567 | −0.757 | −0.565 | −0.699 | −0.568 | −0.758 | −0.542 | −0.718 | −0.568 | −0.753 |

Conventions have been chosen so that the pure 2p lone pair on the oxygen atom of the water molecule belongs to the $B_1$ irreducible representation of the $C_{2v}$ group.

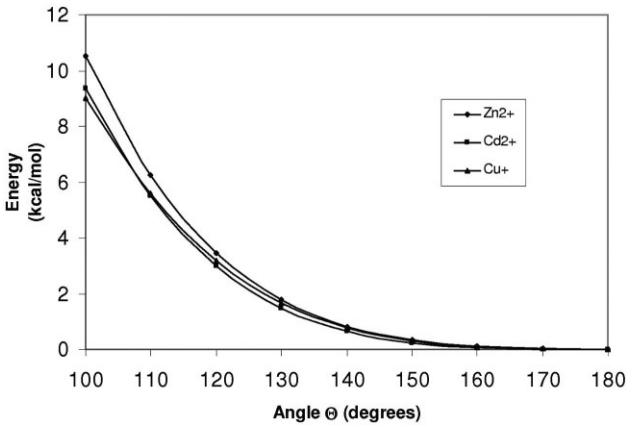


**Figure 5.** Wagging potential energy curves as a function of Θ (see text for definition) for the $Cu^{(I)}$, $Zn^{(II)}$, and $Cd^{(II)}$ water complexes (B3LYP/SDD calculations).

achieved in $Au^+$ and $Hg^{2+}$ by means of relativistic effects. The four remaining complexes might appear as *unpronounced* or *borderline* cases between electrostatic and covalent species: **E** does not dramatically switch toward electrostatic complexes (**E** >> 50%); this might explain why very flat potential energy surfaces are observed when the $\omega$ mode is concerned.

The chemical bonds usually result from subtle compromises between electrostatic and covalent interactions, especially when occurring between a metallic cation and a ligand. Among the six cases investigated here, it is worth to point out $[Au(H_2O)]^+$: with its **E** value limited to less than 4%, and its especially high $E_{rc}^{na}$ value, gold, once again, exhibits a very special character and, still, appears as a better archetype of a relativistic entity than mercury due to the very specific behavior of its $6s_{1/2}$ spinor: energy stabilization and radius contraction.

## Acknowledgments

The four-component computations presented in this article have been supported by the IDRIS (F. 91403, Orsay, France) and CINES (F. 34000 Montpellier, France) national supercomputing centers. The pseudopotential calculations have been performed at the CCR of the University Pierre et Marie Curie (F. 75252, Paris, France).

**Table 11.** CSOV Energy Decompositions (kcal/mol) of the B3LYP/SDD Calculations. "A" Stands for Water and "B" for the Metallic Cation.

| | $[Cu(H_2O)]^+$ | $[Zn(H_2O)]^{2+}$ | $[Cd(H_2O)]^{2+}$ |
|---|---|---|---|
| $\Delta E$ | −43.2 | −106.5 | −82.6 |
| $E_s$ | −60.42 | −90.63 | −74.99 |
| $E_{Pauli}$ | 44.10 | 44.86 | 37.06 |
| $E_1 = E_{FC}$ | −16.32 | −45.77 | −37.93 |
| $E_{polB}$ | −5.99 | −1.93 | −1.68 |
| $E_{polA}$ | −10.50 | −32.14 | −22.25 |
| $E_{ctA\rightarrow B}$ | −8.03 | −24.18 | −19.72 |
| $E_{ctB\rightarrow A}$ | −0.91 | −0.34 | −0.17 |
| $E_2$ | −25.42 | −58.60 | −43.83 |
| $\delta E$ | −1.46 | −2.13 | −0.84 |
| **E** | 37.8% | 43.0% | 45.9% |

## References

1. Lippard, S. J.; Berg, J. M. Principles of Bioinorganic Chemistry; University Science Book: Sausalito, 1994.
2. Orvig, C.; Abrams, M. J. Chem Rev 1999, 99, 2201.
3. Shaw, C. F., III. Chem Rev 1999, 99, 2589.
4. Pyykkö, P.; Desclaux, J. P. Acc Chem Res 1979, 12, 276.
5. Pitzer, K. S. Acc Chem Res 1979, 12, 273.
6. Balasubramanian, K.; Pitzer, K. S. In Ab Initio Methods in Quantum Chemistry; Lawley, K. P., Ed.; John Wiley and Sons Ltd.: New York, 1987, Vol. I.
7. Pyykkö, P. Chem Rev 1988, 88, 563.
8. Pisani, L.; André, J. M.; André, M. C.; Clementi, C. J Chem Educ 1993, 70, 894.
9. Wang, S.; Liu, W.; Schwarz, W. H. E. J Phys Chem A 2002, 106, 795.
10. Heß, B. A., Ed. Relativistic Effects in Heavy-Element Chemistry and Physics; John Wiley and Sons Ltd.: Chichester, 2003.
11. Schwarz, H. Angew Chem Int Ed 2003, 42, 4442.
12. Kaltsoyannis, N. J Chem Soc Dalton Trans 1996, 1, and references therein.
13. Frisch, M. J.; Trucks, G. W.; Schlegel, H. B.; Scuseria, G. E.; Robb, M. A.; Cheeseman, J. R.; Montgomery, J. A., Jr.; Vreven, T.; Kudin, K. N.; Burant, J. C.; Millam, J. M.; Iyengar, S. S.; Tomasi, J.; Barone, V.; Mennucci, B.; Cossi, M.; Scalmani, G.; Rega, N.; Petersson, G. A.; Nakatsuji, H.; Hada, M.; Ehara, M.; Toyota, K.; Fukuda, R.; Hasegawa, J.; Ishida, M.; Nakajima, T.; Honda, Y.; Kitao, O.; Nakai, H.; Klene, M.; Li, X.; Knox, J. E.; Hratchian, H. P.; Cross, J. B.; Bakken, V.; Adamo, C.; Jaramillo, J.; Gomperts, R.; Stratmann, R. E.; Yazyev, O.; Austin, A. J.; Cammi, R.; Pomelli, C.; Ochterski, J. W.; Ayala, P. Y.; Morokuma, K.; Voth, G. A.; Salvador, P.; Dannenberg, J. J.; Zakrzewski, V. G.; Dapprich, S.; Daniels, A. D.; Strain, M. C.; Farkas, O.; Malick, D. K.; Rabuck, A. D.; Raghavachari, K.; Foresman, J. B.; Ortiz, J. V.; Cui, Q.; Baboul, A. G.; Clifford, S.; Cioslowski, J.; Stefanov, B. B.; Liu, G.; Liashenko, A.; Piskorz, P.; Komaromi, I.; Martin, R. L.; Fox, D. J.; Keith, T.; Al-Laham, M. A.; Peng, C. Y.; Nanayakkara, A.; Challacombe, M.; Gill, P. M. W.; Johnson, B.; Chen, W.; Wong, M.W.; Gonzalez, C.; Pople, J. A. Gaussian 03, Revision C.02; Gaussian, Inc.: Wallingford CT, 2004.
14. Dolg, M. In Modern Methods and Algorithms of Quantum Chemistry; Grotendorst, J., Ed.; John von Neumann Institute for Computing: Jülich, 2000; Stoll, H.; Metz, B.; Dolg, M. J Comp Chem 2002, 23, 767.
15. Hay, P. J.; Wadt, W. R. J Chem Phys 1985, 82, 270, 284, and 299.
16. Andrae, D.; Haeussermann, U.; Dolg, M.; Stoll, H.; Preuss, H. Theor Chim Acta 1990, 77, 123.
17. Kuechle, W.; Dolg, M.; Stoll, H.; Preuss, H. Mol Phys 1991, 74, 1245.
18. Ross, R. B.; Powers, J. M.; Atashroo, T.; Ermler, W. C.; LaJohn, L. A.; Christiansen, P. A. J Chem Phys 1990, 93, 6654.
19. LaJohn, L. A.; Christiansen, P. A.; Ross, R. B.; Atashroo, T.; Ermler, W. C. J Chem Phys 1987, 87, 2812.
20. Hurley, M. M.; Pacios, L. F.; Christiansen, P. A.; Ross, R. B.; Ermler, W. C. J Chem Phys 1986, 84, 6840.
21. Faegri, K. Theor Chem Acc 2001, 105, 252.
22. Dirac, a relativistic ab initio electronic structure program, Release

DIRAC04 (2004), written by H. J. Aa. Jensen, T. Saue, and L. Visscher with contributions from V. Bakken, E. Eliav, T. Enevoldsen, T. Fleig, O. Fossgaard, T. Helgaker, J. Laerdahl, C. V. Larsen, P. Norman, J. Olsen, M. Pernpointner, J. K. Pedersen, K. Ruud, P. Salek, J. N. P. van Stralen, J. Thyssen, O. Visser, and T. Winther http://dirac.chem.sdu.dk.
23. Saue, T.; Helgaker, T. J Comp Chem 2002, 23, 814.
24. Fossgaard, O.; Gropen, O.; Corral Valero, M.; Saue, T. J Chem Phys 2003, 118, 10418.
25. Lévy–Leblond, J. M. Commun Math Phys 1967, 6, 286.
26. Visscher, L.; Saue, T. J Chem Phys 2000, 113, 3996, and references therein.
27. Visscher, L.; Dyall, K. G. At Data Nucl Data Tabl 1997, 67, 207.
28. Douglas, M.; Kroll, N. M. Ann Phys (NY) 1974, 82, 89.
29. Heß, B. A. Phys Rev A 1985, 32, 756.
30. Heß, B. A. Phys Rev A 1986, 33, 3742.
31. Jansen, B.; Heß, B. A. Phys Rev A 1989, 39, 6016.
32. (a) Carpenter, J. E.; Weinhold, F. J Mol Struct (Theochem) 1988, 169, 41; (b) Carpenter, J. E. PhD thesis, University of Wisconsin, Madison, WI, 1987; (c) Foster, J. P.; Weinhold, F. J Am Chem Soc 1980, 102, 7211; (d) Reed, A. E.; Weinhold, F. J Chem Phys 1983, 78, 4066; (e) Reed, A. E.; Weinhold, F. J Chem Phys 1985, 83, 1736; (f) Reed, A. E.; Weinstock, R. B.; Weinhold, F. J Chem Phys 1985, 83, 735; (g) Reed, A. E.; Curtiss, L. A.; Weinhold, F. Chem Rev 1988, 88, 899; (h) Glendening, E. D.; Reed, A. E.; Carpenter, J. E. Weinhold, F. NBO Version 3.1.
33. Boys, S. F.; Bernardi, F. Mol Phys 1970, 19, 553.
34. Hobza, P.; Zahradnik, R. Chem Rev 1988, 88, 871.
35. Dupuis, M.; Marquez, A.; Davidson, E. R. "HONDO95.3," Quantum Chemistry Program Exchange (QCPE) Indiana University, Bloomington, IN.
36. Holland, P. M.; Castelman, A. W., Jr. J Chem Phys 1982, 76, 4195.
37. El Aribi, H.; Shoeib, T.; Ling, Y.; Rodriquez, C. F.; Hopkinson, A. C.; Siu, K. W. M. J Phys Chem A 2002, 106, 2908.
38. Koizumi, H.; Larson, M.; Muntean, F.; Armentrout, P. B. Int J Mass Spectrosc 2003, 228, 221.
39. Chattaraj, P. K.; von Ragué Schleyer, P, J Am Chem Soc 1994, 116, 1067.
40. Martinez, J. M.; Pappalardo, R. R.; Marcos, E. S. J Phys Chem A 1997, 101, 4444.
41. Ma, N. L. Chem Phys Lett 1998, 297, 230.
42. Feller, D.; Glendening, E. D.; de Jong, W. A. J Chem Phys 1999, 110, 1475.
43. Boutreau, L.; Leon, E.; Luna, A.; Toulhoat, P.; Tortajada, J. Chem Phys Lett 2001, 338, 74.
44. Widmer–Cooper, A. N.; Lindoy, L. F.; Reimers, J. R. J Phys Chem A 2001, 105, 6567.
45. Fox, B. S.; Beyer, M. K.; Bondybey, V. E. J Am Chem Soc 2002, 124, 13613.
46. Lee, E. C.; Lee, H. M.; Tarakeshwar, P.; Kim, K. S. J Chem Phys 2003, 119, 7725.
47. Chang, C. M. J Mol Struct (Theochem) 2003, 622, 249.
48. Gresh, N.; Giessner–Prettre, C. New J Chem 1997, 21, 279.
49. Antušek, A.; Urban, M.; Sadlej, A. J. J Chem Phys 2003, 119, 7247.
50. Barysz, M.; Leszczyński, J.; Bilewicz, A. Phys Chem Chem Phys 2004, 6, 4553.
51. Schröder, D.; Hrušák, J.; Hertwig, R. H.; Koch, W.; Schwerdtfeger, P.; Schwarz, H. Organometallics 1995, 14, 312.
52. Schröder, D.; Schwarz, H.; Hrušák, J.; Pyykkö, P. Inorg Chem 1988, 37, 624.
53. Poisson, L.; Pradel, P.; Lepetit, F.; Réau, F.; Mestdagh, J.-M.; Visticot, J.-P. Eur Phys J 2001, D14, 89.
54. Poisson, L.; Lepetit, F.; Mestdagh, J.-M.; Visticot, J.-P. J Phys Chem A 2002, 106, 5455.
55. Poisson, L.; de Pujo, P.; Brenner, V.; Derepas, A.-L.; Dognon, J.-P.; Mestdagh, J.-M. J Phys Chem A 2002, 106, 1714.
56. Hrušák, J.; Schröder, J.; Schwarz, H. Chem Phys Lett 225 1994, 416.
57. Hertwig, J. H.; Hrušák, J.; Schröder, D.; Koch, W.; Schwarz, H. Chem Phys Lett 1995, 236, 194.
58. Hrušák, J.; Hertwig, R. H.; Schröder, D.; Schwerdtfeger, P.; Koch, W.; Schwarz, H. Organometallics 1995, 14, 1284.
59. (a) Nesbitt, D. J.; Naaman, R. J Chem Phys 1989, 91, 3801, and in references therein; (b) Saykally, R. J. Science 1988, 239, 157; (c) Herzberg, G. Molecular Spectra and Molecular Structure. II—Infrared and Raman Spectra of Polyatomic Molecules; Van Nostrand: Princeton, NJ, 1945; (d) Kroto, H. W. Molecular Rotation Spectra; Wiley: New York, 1975; (e) Wilson, E. B., Jr.; Decius, J. C.; Cross, P. C. Molecular Vibrations. The Theory of Infrared and Raman Vibrational Spectra; McGraw-Hill: New York, 1955.
60. Probst, M. M. J Mol Struct (Theochem) 1992, 253, 275.
61. Sinha, S. P. Inorg React Mech 2000, 2, 33.
62. Soldán, P.; Lee, E. P. F.; Wright, T. G. J Phys Chem A 2002, 106, 8619.
63. Visscher, L.; Dyall, K. G. J Chem Phys 1996, 104, 9040.
64. Visscher, L.; Styszyñski, J.; Nieuwpoort, W. C. J Chem Phys 1996, 105, 1987.
65. de Jong, W. A.; Styszyñski, J.; Visscher, L.; Nieuwpoort, W. C. J Chem Phys 1998, 108, 5177.
66. Pyykkö, P. Angew Chem Int Ed 2002, 41, 3573.
67. Pyykkö, P. Angew Chem Int Ed 2004, 43, 4412.
68. Duval, M. C.; Soep, B. J Phys Chem 1991, 95, 9075, and references therein.
69. Duval, M. C.; Soep, B.; van Zee, R. D.; Bosma, W. B.; Zwier, T. S. J Chem Phys 1988, 88, 2148, and references therein.
70. Callear, A. B. Chem Rev 1987, 87, 335, and references therein.
71. Kollman, P.; McKelvey, J.; Johansson, A.; Rothenberg, S. J Am Chem Soc 1975, 97, 955.
72. Bagus, P. S.; Hermann, K.; Bauschlicher, C. W., Jr. J Chem Phys 1984, 80, 4378.
73. Bagus, P. S.; Illas, F. J Chem Phys 1992, 96, 463.
74. Morokuma, K. J Chem Phys 1971, 55, 1236.
75. Kitaura, K.; Morokuma, K. Int J Quantum Chem 1976, 10, 325.
76. Gordon, M. S.; Jensen, J. H. In Encyclopaedia of Computational Chemistry; von Ragué Schleyer, P., Ed.; John Wiley and Sons Ltd.: Chichester, 1998, p. 3198–3214, vol. V.
77. Stevens, W. J.; Fink, W. Chem Phys Lett 1987, 139, 15.
78. Neyman, K. M.; Ruzankin, S. Ph.; Rösch, N. Chem Phys Lett 1995, 246–546.
79. Chung, S. C.; Kruger, S.; Ruzankin, S. Ph.; Pacchioni, G.; Rösch, N. Chem Phys Lett 1996, 248, 109.
80. Márquez, A. M.; López, N.; García–Hernández, M.; Illas, F. Surface Sci 1999, 442, 463.
81. Ricca, A.; Bauschlicher, C. W. J Phys Chem A 2002, 106, 3219.
82. Piquemal, J.-P.; Marquez, A.; Parisel, O.; Giessner–Prettre, C. J Comp Chem 2005, 26, 1052.
83. Gresh, N.; Garmer, D. R. J Comp Chem 1996, 17, 1481.
84. Peschke, M.; Blades, A. T.; Kebarle, P. J Am Chem Soc 2000, 122, 10440.
85. Smith, G. D.; Bell, R.; Borodin, O.; Jaffe, R. L. J Phys Chem A 2001, 105, 6506.
86. Pavlov, M.; Siegbahn, P. E. M.; Sandström, M. J Phys Chem A 1998, 102, 219.
87. Garmer, D. R.; Gresh, N. J Am Chem Soc 1994, 116, 3556.
88. Peschke, M.; Blades, A. T.; Kebarle, P. Int J Mass Spectrosc 1999, 185–187, 685.

89. Bock, C. W.; Katz, A. K.; Glusker, J. P. J Am Chem Soc 1995, 117, 3754.
90. Lee, E. P. F.; Soldán, P.; Wright, T. G. J Phys Chem A 2001, 105, 8510.
91. Rosi, M.; Bauschlicher, C. W., Jr. J Chem Phys 1989, 90, 7264; 1989, 92, 1876.
92. Cheng, M.-J.; Hu, C.-H.; Yeh, C.-S. J Phys Chem A 2002, 106, 11570.
93. Bauschlicher, C. W., Jr.; Langhoff, S. R.; Partridge, H. J Chem Phys 1991, 94, 2068.
94. Hoyau, S.; Ohanessian, G. Chem Phys Lett 1997, 280, 266.
95. Ducéré, J.-M.; Goursot, A.; Berthomieu, D. J Phys Chem A 2005, 109, 400.
96. Luna, A.; Alcamí, M.; Mó, O.; Yáñez, M. Chem Phys Lett 2000, 320, 129.
97. Ghanty, T. K.; Davidson, E. R. Int J Quantum Chem 2000, 77, 291.
98. Lynch, B. J.; Truhlar, D. G. Chem Phys Lett 2002, 361, 251.
99. Dalleska, N. F.; Honma, K.; Sunderlin, L. S.; Armentrout, P. B. J Am Chem Soc 1994, 116, 3519.